TOXICOLOGICAL SCIENCES **131(1)**, 116–127 (2013)
doi:10.1093/toxsci/kfs288
Advance Access publication September 26, 2012

Quantitative Analysis of the Interaction of Constitutive Androstane Receptor with Chemicals and Steroid Receptor Coactivator 1 Using Surface Plasmon Resonance Biosensor Systems: A Case Study of the Baikal Seal (*Pusa sibirica*) and the Mouse

Pham Thi Dau,*[,1] Hiroki Sakai,* Masashi Hirano,* Hiroshi Ishibashi,* Yuki Tanaka,† Kenji Kameda,† Takahiro Fujino,† Eun-Young Kim,‡[,2] and Hisato Iwata*[,2,3]

*Center for Marine Environmental Studies (CMES), Ehime University, Matsuyama 790–8577, Japan; †Department of Bioscience, Integrated Center for Sciences (INCS), Ehime University, Toon 791-0295, Japan; and ‡Department of Life and Nanopharmaceutical Science and Department of Biology, Kyung Hee University, Hoegi-Dong, Dongdaemun-Gu, Seoul 130–701, Korea

[1]Research and Development Center for Petroleum Safety and Environment (CPSE), Vietnam Petroleum Institute (VPI), G1 Building, Thanh Da Hotel, 27 Ward, Binh Thanh District, Ho Chi Minh City, Vietnam.
[2]These authors contributed equally to this study.
[3]To whom correspondence should be addressed at Laboratory of Environmental Toxicology, Center for Marine Environmental Studies (CMES), Ehime University, Matsuyama 790-8577, Japan. Fax: +81-89-927-8172. E-mail: iwatah@agr.ehime-u.ac.jp.

Received May 23, 2012; accepted September 18, 2012

The constitutive androstane receptor (CAR) not only displays a high basal transcriptional activity but also acts as a ligand-dependent transcriptional factor. It is known that CAR exhibits different ligand profiles across species. However, the mechanisms underlying CAR activation by chemicals and the species-specific responses are not fully understood. The objectives of this study are to establish a high-throughput tool to screen CAR ligands and to clarify how CAR proteins from the Baikal seal (bsCAR) and the mouse (mCAR) interact with chemicals and steroid receptor coactivator 1 (SRC1). We developed the surface plasmon resonance (SPR) system to assess quantitatively the interaction of CAR with potential ligands and SRC1. The ligand-binding domain (LBD) of bsCAR and mCAR was synthesized in a wheat germ cell–free system. The purified CAR LBD was then immobilized on the sensor chip for the SPR assay, and the kinetics of direct interaction of CARs with ligand candidates was measured. Androstanol and androstenol, estrone, 17β-estradiol, TCPOBOP, and CITCO showed compound-specific but similar affinities for both CARs. The CAR-SRC1 interaction was ligand dependent but exhibited a different ligand profile between the seal and the mouse. The results of SRC1 interaction assay accounted for those of our previous *in vitro* CAR-mediated transactivation assay. *In silico* analyses also supported the results of CAR-SRC1 interaction; there is little structural difference in the ligand-binding pocket of bsCAR and mCAR, but there is a distinct discrimination in the helix 11 and 12 of these receptors, suggesting that the interaction of ligand-bound CAR and SRC1 is critical for determining species-specific and ligand-dependent transactivation over the basal activity. The SPR assays demonstrated a potential as a high-throughput screening tool of CAR ligands.

Key Words: **Baikal seal; constitutive androstane receptor; direct ligand binding; steroid receptor coactivator 1; surface plasmon resonance.**

The constitutive androstane receptor (CAR), which is categorized as nuclear receptor subfamily 1, group I, and member 3, acts as a ligand-dependent transcriptional factor, and also this receptor displays a high basal transcriptional activity even in the absence of ligands (Baes *et al*., 1994; Masi *et al*., 2009). Upon stimulation of ligands, CAR can be translocated from the cytoplasm into the nucleus (Kanno and Inouye, 2008; Kawamoto *et al*., 1999). CAR then forms a heterodimer with retinoid X receptor (RXR) α and binds to a specific DNA sequence, phenobarbital (PB)–responsive enhancer module in the upstream of target genes (Honkakoski *et al*., 1998). The heterodimer complex recruits steroid receptor coactivator 1 (SRC1), a member of the SRC/p160 coactivator family (Leo and Chen, 2000), through helix H12 in the activation function 2 (AF2) domain of CAR (Jyrkkärinne *et al*., 2005; Mäkinen *et al*., 2003). Consequently, this complex is able to upregulate the transcription of CAR target genes (Honkakoski *et al*., 1998; Kawamoto *et al*., 1999), including cytochrome P450 2B, 2C, and 3A, uridine diphosphate glucuronosyltransferases, sulfotransferases, glutathione *S*-transferases, and transporters (Assem *et al*., 2004; Wyde *et al*., 2003). These genes participate in the metabolism and excretion of PB-like xenobiotic compounds. Together with these molecular events, they can regulate physiological conditions through the metabolism of endogenous

compounds such as steroid and thyroid hormones, bile acids, and bilirubin (Beilke *et al*., 2009; Huang *et al*., 2003; Qatanani *et al*., 2005). They are also involved in the synthesis/metabolism of glucose and lipid (Dong *et al*., 2009). Several studies have shown that CAR activation by PB-like compounds is associated with liver tumor development and hepatocarcinogenesis in rodents (Huang *et al*., 2005; Yamamoto *et al*., 2004). Hence, identifying and quantifying PB-type chemicals that can modulate the CAR-mediated signaling pathways may give an insight into the risk and effects of these chemicals in humans and wildlife.

Studies on the CAR signaling pathway have reported that there are distinct species differences in ligand profiles between humans and rodents (Jyrkkärinne *et al*., 2005; Kawamoto *et al*., 2000; Moore *et al*., 2000). A hepatomitogen TCPOBOP (1,4-bis-[2-(3,5-dichloropyridyloxy)]benzene) is a potent mouse CAR (mCAR) agonist (Tzameli *et al*., 2000) but is not an agonist for human CAR (hCAR) (Moore *et al*., 2000). In contrast, an imidazothiazole derivative, CITCO (6-(4-chlorophenyl)imidazo [2,1-b][1,3] thiazole-5-carbaldehyde *O*-(3,4-dichlorobenzyl) oxime) can activate hCAR (Maglich *et al*., 2003) but has less effect on mCAR (Sakai *et al*., 2006). It has also been demonstrated that a limited number of PB-like compounds can modulate the activity of CAR through direct or indirect interaction with ligand-binding domain (LBD) of this receptor (Kawamoto *et al*., 1999; Moore *et al*., 2000). Androstanol efficiently competed with [^{3}H] clotrimazole for binding to hCAR, but TCPOBOP, which showed no effect on hCAR transactivation, displayed no competition with [^{3}H] clotrimazole (Moore *et al*., 2000). Interestingly, PB that could deactivate hCAR did not compete with [^{3}H] clotrimazole, indicating no direct interaction of PB and hCAR (Moore *et al*., 2000). Another study revealed that TCPOBOP binds to mCAR and consequently regulates transactivation (Suino *et al*., 2004). Nevertheless, little is known about the interaction of most of the ligands with CAR protein and their kinetics.

The Baikal seal (*Pusa sibirica*), an endemic species and a top predator in the Lake Baikal, Russia, is contaminated with persistent organic pollutants (Imaeda *et al*., 2009; Iwata *et al*., 2004). Our previous studies have successfully isolated a complementary DNA (cDNA) of CAR from the Baikal seal (bsCAR) and investigated the *in vitro* transactivation potencies of bsCAR by PB-type chemicals (Sakai *et al*., 2006, 2009). The bsCAR responded to some PB-type chemicals in a compound-specific manner. Intriguingly, the ligand profile of bsCAR was different from that of mCAR, suggesting the difference in the ligand-binding potencies across the species. However, the mechanism underlying the species-specific responses of CAR to chemicals is not yet well understood; there exists a requirement for a more comprehensive approach to screen potential CAR ligands in these species.

Surface plasmon resonance (SPR) biosensor is a multiplex optical device that monitors bimolecular interactions in real time without labeling of molecules. It is a novel analytical instrument used to measure the interaction of molecules with immobilized molecular targets. This instrument is suitable for high-throughput screening assays because of its capability for simultaneous measurement of various individual interactions and has been used for monitoring the chemical-receptor interactions (Rich *et al*., 2002).

The objectives of this study are to establish a high-throughput tool to screen CAR ligands and to clarify how CAR proteins from the Baikal seal and the mouse interact with chemicals and SRC1. In this study, we developed SPR bioassay systems for screening the interaction of CAR proteins with PB-type compounds. We synthesized the LBD of bsCAR and mCAR with an *in vitro* wheat germ cell–free system (Endo and Sawasaki, 2003). The binding affinities of candidate chemicals with CAR LBDs were measured with the SPR system. Furthermore, to confirm the effect of ligands on the interaction of CAR with SRC1, the ligand-treated CAR LBD and SRC1 interaction was also monitored. Based on these SPR assays, the ligand profile of bsCAR and mCAR was compared. In addition, 3-dimensional models of bsCAR and mCAR were constructed by an *in silico* homology modeling and were used to account for the differences in the ligand-dependent transactivation potencies across the species.

MATERIALS AND METHODS

Chemicals. Dimethyl sulfoxide (DMSO), androstanol, androstenol, estrone, 17β-estradiol, bisphenol A (BPA), and TCPOBOP were purchased from Sigma-Aldrich, Inc. (St Louis, MO). CITCO was purchased from Biomol (Plymouth Meeting, PA). Cholic acid (CA), chenodeoxycholic acid (CDCA), deoxycholic acid (DCA), and lithocholic acid (LCA) were obtained from Wako (Osaka, Japan). The structures of these chemicals are shown in Supplementary figure S1.

Cloning and protein synthesis. The sequences of LBD encoding residues 107–348 of bsCAR and 117–358 of mCAR were amplified by PCR with specific primer sets containing restriction enzyme *Xho*I and *Not*I recognition sites. Amplicons were then treated with the restriction enzymes and were subcloned into pEU-E01-GST-N2 and pEU-E01-His-N2 expression vectors containing a glutathione *S*-transferase (GST)- or histidine (His)-tag region, respectively (CellFree Sciences Co., Ltd., Matsuyama, Japan). CAR LBDs were synthesized with the Robotic Protein Synthesizer ProtemistDT (GST-fusion protein) or DTII (His-fusion protein) following an *in vitro* cell-free protein synthesis system using wheat germ ribosomal RNA (CellFree Sciences) (Sawasaki *et al*., 2002). The transcription mixture (250 µl), containing 25 µg of the plasmid DNA, 80mM HEPES-KOH (pH 7.8), 16mM magnesium acetate, 2mM spermidine, 10mM dithiothreitol (DTT), 2.5mM each of nucleoside triphosphates, 250 U of SP6 RNA polymerase, and 250 U of RNasin (Promega), was incubated at 37°C for 6 h. The translation mixture, including the transcription solution, was then supplemented with 250 µl of wheat germ cell extract WEPRO 1240G or 7240H (CellFree Sciences) for the GST- or His-fusion proteins, respectively, and further with 2 µl of 20 mg/ml creatine kinase. The substrate mixture (5.5 ml), containing 30mM HEPES-KOH, pH 7.8, 100mM potassium acetate, 2.7mM magnesium acetate, 0.4mM spermidine, 2.5mM DTT, 0.3mM amino acid mix, 1.2mM ATP, 0.25mM GTP, and 16mM creatine phosphate (CellFree Sciences), was added to the translation mixture and then incubated for 20 h at 17°C.

Crude solutions of synthesized GST-bsCAR and/or -mCAR LBDs were centrifuged at 4°C and 15,000 g for 15 min. The supernatant was then loaded on a GST affinity column (GE Healthcare) according to the manufacturer's instruction. The purified GST-CAR LBD proteins were dialyzed with HEPES buffer (10mM HEPES, pH 7.8, 3mM EDTA, 4mM DTT, 0.005% Tween 20) at 4°C overnight. The CAR LBDs were further purified by ion exchange chromatography with a Hi Trap Q HP column (GE Healthcare). GST-bsCAR and -mCAR LBDs were eluted using the above HEPES buffer with a gradient solution of

NaCl (from 0 up to 1M). His-CAR LBDs were purified with a Ni Sepharose High Performance Column (GE Healthcare) following the manufacturer's instruction. The column on which the crude solution was loaded was washed with a buffer (20mM phosphate buffer, 300mM NaCl, 50mM imidazole, pH 7.5). His-CAR LBDs were then eluted with an elution buffer (20mM phosphate buffer, 300mM NaCl, 500mM imidazole, pH 7.5) and dialyzed against PBS using Mini Dialysis Kit (GE Healthcare).

Fractions containing GST- or His-CAR LBDs were separated by SDS-PAGE, and the CAR LBDs were detected by Coomassie brilliant blue staining. Purified proteins were preconcentrated by centrifugation at 14,000 g and 4°C using Microcon Ultracel (Millipore). Contents of concentrated proteins were determined using Agilent Protein 230 Kit (Agilent Technologies).

Nontagged human SRC1 receptor-interaction domain (SRC1-RID) which contains three receptor-interaction domains (LXXLL) was purchased from ProteinOne (Bethesda, MD).

Interaction of chemicals with CAR LBD. The binding of candidate chemicals with CAR LBD was detected with ProteOn XPR36 (Bio-Rad Laboratories, Inc.). The optimal conditions of pH for immobilization of His-bsCAR and mCAR LBDs on the GLH sensor chip were initially determined. The CAR LBDs were diluted with 10mM sodium acetate buffer in a series of pH 4.0, 4.5, 5.0, and 5.5 and injected sequentially at a flow rate of 25 µl/min for 1 min. The CAR LBDs were immobilized under optimal conditions using Amine Coupling Kit (Bio-Rad Laboratories, Inc.) as explained in a previous report (Turner *et al*., 2008) with some modifications. The selected channels on the carboxylated sensor chip (Bio-Rad Laboratories, Inc.) were activated by a 1:1 (vol/vol) mixture of 50mM N-hydroxysuccinimide (NHS) and 200mM 1-ethyl-3-(3-dimethylaminopropyl)carbodiimide hydrochloride (EDC) at a flow rate of 30 µl/min for 5 min. Following activation, the protein solution that was prepared in 10mM sodium acetate buffer with the optimal pH (Supplementary table S1) was immediately injected into each of the activated channels at a flow rate of 25 µl/min. The protein-fixed channels were then deactivated immediately by ethanolamine hydrochloride (1M, pH 8.5) at a flow rate of 30 µl/min for 5 min. The amount of immobilized protein was measured as a response unit (RU) relative to the baseline signal before activation. HEPES-buffer saline (pH 7.4), including 10mM HEPES, 150mM NaCl, and 0.005% Tween 20, was used as a running buffer for the immobilization (Rich *et al*., 2002). PBS (20mM Na_2HPO_4, 150mM NaCl, 1mM DTT, 0.005% Tween 20, pH 7.4, and 5% DMSO) was used as the running buffer throughout the kinetic processes (Rich *et al*., 2002; Turner *et al*., 2008). Stock solution of each chemical as an analyte was prepared in DMSO and diluted into a series of concentrations with the running buffer to detect the direct binding with immobilized His-CAR LBDs. Final concentration of DMSO for each analyte solution was adjusted to 5% vol/vol. The prepared analytes were injected into the six analyte channels under the conditions shown in Table 1. The dissociation of analyte from the sensor chip of ProteOn XPR36 was carried out by injecting a running buffer for 10 min. All experiments were performed at 25°C at least thrice to check reproducibility.

Interaction of ligand-treated CAR LBD with SRC1. CAR-LBD/SRC1-RID interaction was analyzed by using Biacore 2000 (GE Healthcare). Immobilization of SRC1-RID was performed onto the hydrophilic carboxymethylated dextran matrix of the CM5 sensor chip (GE Healthcare) using Amine Coupling Kit (GE Healthcare). Initially, the flow cell of SPR sensor chip was activated by a 1:1 (vol/vol) mixture of 50mM NHS and 200mM EDC for 7 min. Five micrograms per milliliter of SRC1-RID protein diluted by 10mM sodium acetate buffer (pH 5.5) was then injected with a flow rate of 5 µl/min using an injection program. Finally, the sensor chip was deactivated with 1M ethanolamine-HCl (pH 8.5) for 7 min to block any remaining activated residues. Depending on the buffer profile of fractions eluted from ion exchange chromatography, the same running buffers were prepared to detect the interaction between SRC1 and ligand-treated CAR LBD. The HEPES buffers (10mM HEPES pH 7.8, 3mM EDTA, 4mM DTT, 0.005% Tween 20) with 285 and 373mM of NaCl were used for GST-bsCAR LBD and GST-mCAR LBD, respectively. Five percentage of DMSO was added to the running buffer to make the same solvent concentration of the running buffer as the analyte solution. The interaction assay between SRC1 and CAR LBD in the presence of a variety of CAR ligands was performed with 250nM of GST-CAR LBD. The mixture of CAR LBD and a single test chemical was incubated at 25°C for 1 h and was then injected at a flow rate of 20 µl/min. Association and dissociation of CAR-LBD/SRC1-RID were performed for 2 min and 5 min, respectively. Immobilized SRC1-RID protein was regenerated with an injection of 10mM NaOH for 30 s. Activity of SRC1-RID after regeneration was confirmed by repeating analyses using the same analyte solution. All experiments were performed at 25°C and at least twice to check the reproducibility.

Computational modeling. The homology modeling for the CAR LBD and the *in silico* analysis of the interaction potential between ligands and the CAR LBD were performed using the programs of Molecular Operating Environment (MOE) (Chemical Computing Group Inc., Montreal, QB, Canada). The crystal structures of hCAR and mCAR LBDs were obtained from Protein Data Bank (PDB) entry 1xvp (Xu *et al*., 2004) and 1xls (Suino *et al*., 2004), respectively. The crystal structure of hCAR has been constructed based on CAR/RXR LBD heterodimer bound to CITCO and a SRC1 peptide and that of mCAR has been based on CAR/RXR LBD heterodimer bound to TCPOBOP and 9cis-retinoic

TABLE 1
Molecular Characteristics of Tested Chemicals and the SPR Analytical Conditions for the Interaction of Chemicals with Baikal Seal and Mouse CAR LBDs

Chemical	Molecular formula	Molecular weight (g/mol)	Molar volume (cm^3/mol)	Molecular volume (Å^3)	Analytical conditions		
					Concentration (µM)	Flow rate (µl/min)	Contact time (s)
Androstanol	$C_{19}H_{32}O$	276.5	271.1	306.2	0, 1.2, 3.7, 11, 33, 100	25	240
Androstenol	$C_{19}H_{30}O$	274.4	264.4	n.a.	0, 1.2, 3.7, 11, 33, 100	25	240
Estrone	$C_{18}H_{22}O_2$	270.4	232.1	n.a.	0, 1.2, 3.7, 11, 33, 100	25	240
17β-Estradiol	$C_{18}H_{24}O_2$	272.4	232.6	277.5	0, 2.5, 7.4, 22, 67, 200	25	240
TCPOBOP	$C_{16}H_8N_2O_2Cl_4$	402.1	264.9	318.3	0, 1.2, 3.7, 11, 33, 100	100	60
CITCO	$C_{19}H_{12}N_3OCl_3S$	436.7	293.4	360.6	0, 0.3, 0.7, 2.2, 6.7, 20	25	240
BPA	$C_{15}H_{16}O_2$	228.3	199.6	238.0	0, 19, 38, 75, 150, 300	25	240
CA	$C_{24}H_{40}O_5$	408.6	344.8	n.a.	0, 6.3, 19, 56, 167, 500	25	240
CDCA	$C_{24}H_{40}O_4$	392.6	347.9	n.a.	0, 0.6, 1.9, 5.6, 16.7, 50	25	240
DCA	$C_{24}H_{40}O_4$	392.6	347.9	n.a.	0, 0.6, 1.9, 5.6, 16.7, 50	25	240
LCA	$C_{24}H_{40}O_3$	376.6	350.9	398.6	0, 0.6, 1.9, 5.6, 16.7, 50	25	240

Note. Molecular volume was cited from http://www.chemspider.com/. Molecular volume was estimated by the method of MD simulation described in Materials and Methods section. n.a., no data is available because no simulation was performed.

acid and a TIF2 peptide. To build a homology model of bsCAR LBD, 1xvp was taken as a template. The amino acid sequence of bsCAR LBD was aligned with that of 1xvp to yield a readily superimposable three-dimensional model. The structure of bsCAR LBD in the absence of the ligand was optimized by AMBER99 force field with an energy gradient of 0.05 (Wang *et al*., 2000). The obtained models of bsCAR and mCAR LBDs were prepared with Protonate 3D program by adjusting the protonation state to pH 7.0 of the running buffer in which the ligand-CAR interaction was monitored. These structures were then used to identify the ligand-binding sites using MOE Alpha Site Finder. Chemical structures including TCPOBOP and androstenol were constructed using the ISIS/Draw program (MDL Information Systems Inc., San Leandro, CA) and rendered and minimized with the MMFF94x force field in MOE (Halgren, 1996). To calculate the molecular volume of some tested chemicals in aqueous phase, molecular dynamics (MD) experiments were conducted using the MMFF94x force field with gas-phase electrostatics. For MD simulations, the Nose-Hoover-Andersen method was used as a NVT ensemble. The systems were subjected to 20 ps heating and equilibration from 100 to 300 K, followed by 1 ns simulation at 300 K with 2 fs time steps. The molecular volumes of the resulting ligand structures were calculated by the AtomRegion program using a grid space of 0.1 Å. The possible docking of TCPOBOP and androstenol was searched with the ASEDock program. All the algorithms of ASEDock were coded using MOE's powerful vector language SVL (Scientific Vector Language). Existing features implemented in MOE were fully applied to realize the functions of ASEDock. A total of 250 conformations for each chemical were generated by Lowmode MD. The ligand conformations were subjected to energy minimization using MMFF94x force field. The most stable binding modes of ligands with the CARs were determined on the basis of the lowest U_total value (kcal/mol). The critical amino acids for the ligand interaction were determined by the ligand interaction module of MOE.

Data analysis. Data of chemical binding to CAR LBD were analyzed using ProteOn ManagerTM 2.1.1 software. Binding curves were processed by aligning baseline and start injection signals and by subtracting signals of an activated and blocked reference channel from those of the CAR-immobilized channels. The binding affinity was evaluated by equilibrium dissociation constant (K_D) drawn from responses of the six graded analyte concentrations. The responses were fitted to a simple bimolecular equilibrium model at 50% saturation response. For the chemical for which a maximum plateau was not achieved from dose-dependent responses under the assay conditions, no K_D was obtained. Significance of differences in each K_D between bsCAR and mCAR was determined by Student's *t*-test ($p < 0.05$). The interactions of ligand-treated CAR-LBD and SRC1-RID were analyzed using BiaEvaluation version 4.1 (GE Healthcare).

RESULTS

Protein Expression by an In Vitro Wheat Germ Cell–Free System. To carry out the kinetic analyses of the interaction of CAR LBDs with potential ligands and with SRC1, the GST- and His-tagged CAR LBDs of the Baikal seal and the mouse were synthesized with an *in vitro* wheat germ cell–free system and were then subjected for purification through affinity columns (Fig. 1). The SDS-PAGE demonstrated that we could obtain purified CAR LBDs. The yield of bsCAR and mCAR was about 100 µg/ml of the *in vitro* translation solution.

Interaction of Chemicals with CAR LBD. To define the direct binding capacity of structurally diverse compounds to CARs, the SPR biosensor was designed for the ligand-binding assay with ProteOn XPR36. His-tagged bsCAR and mCAR LBD proteins were initially immobilized on the SPR sensor chip. For the immobilization onto ProteOn GLH sensor chip, factors such as pH of protein dilution buffer, running buffer composition, flow rate, and contact time were optimized. We found that pH of protein dilution buffer was the most important factor because it can potentially alter the net charge, the conformation, and the activity of proteins. The immobilized amount of CAR LBD protein under various pH conditions of sodium acetate buffer as the protein dilution buffer was determined from the average SPR response of the six channels. The results are shown in Supplementary table S1. Maximum immobilization of both His-tagged bsCAR and mCAR LBDs occurred at pH 4.0 of sodium acetate buffer (130 and 77 RU, respectively), which is lower than the isoelectric point (pI) of the His-tagged CAR LBDs. At higher pH (4.5, 5.0, and 5.5) of the sodium acetate buffer, the amount of immobilized CAR protein decreased, probably due to loss of the net positively charged amino acid residues that would cause the poor electrostatic attraction between the protein and the negatively charged

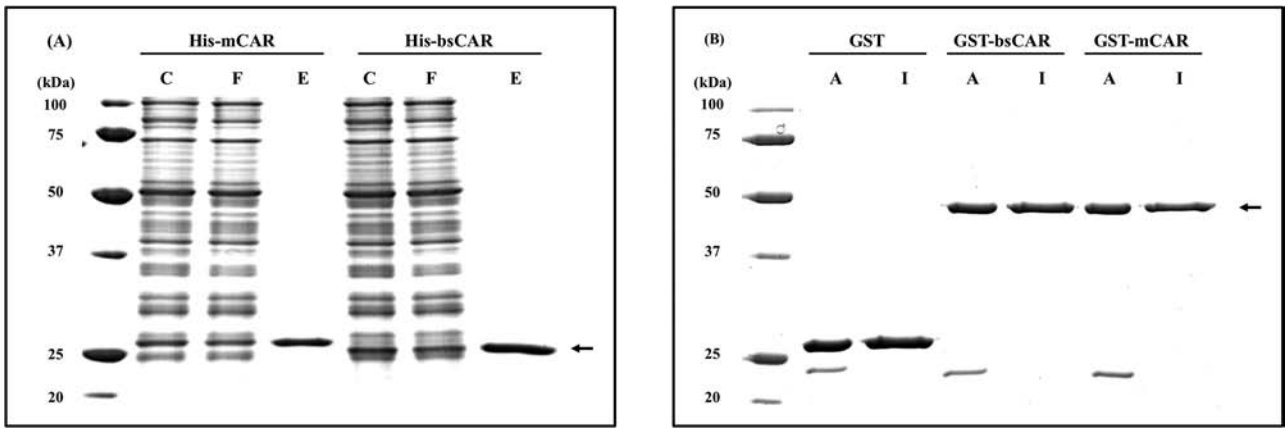

FIG. 1. SDS-PAGE analysis of CAR LBD proteins expressed in the wheat germ cell–free system. (A) His-CAR LBDs were purified by the affinity chromatography with a Ni Sepharose High Performance Column. (B) GST and GST-fusion CAR LBDs were purified by the affinity chromatography with Glutathione Sepharose 4B Column (lane A) and further by the ion exchange chromatography with HiTrap Q HP Column (lane I). Arrow indicates the bands from purified CAR LBD. C, Crude solution; F, Flow-through solution; E, Eluted solution.

TABLE 2
Interspecies Comparison of Ligand Binding, SRC1 Interaction, and Transactivation Potencies of Baikal Seal and Mouse CAR LBDs

	Baikal seal			Mouse		
Chemical	Ligand binding assay K_D (μM)*	SRC1 interaction assay	Transactivation assay	Ligand binding assay K_D (μM)*	SRC1 interaction assay	Transactivation assay
Androstanol	26 ± 3.8	→	→	26 ± 9.6	↓↓	↓↓
Androstenol	16 ± 6.1	→	→	25 ± 6.9	↓↓	↓↓
Estrone	8.7 ± 5.2	→	→	7.8 ± 3.8	↑	↑
17β-Estradiol	34 ± 9.2	→	→	39 ± 9.5	↑	↑
TCPOBOP	12 ± 3.4	→	→	17 ± 4.9	↑↑↑	↑↑↑
CITCO	1.9 ± 0.2	↑↑	↑↑	2.2 ± 0.6	↑	↑
BPA	NSB	ND	ND	NSB	ND	ND
CA	NSB	ND	→	NSB	ND	→
CDCA	NSB	ND	↑	NSB	ND	↑
DCA	NSB	ND	↑	NSB	ND	↑
LCA	NSB	↓	↑	NSB	↓	↑

Note. NSB, Nonspecific binding; ND, not determined; *, Dissociation constant (μM); ↑, activation; ↓, repression; →, no effect.
Student's *t*-test showed no statistical difference in K_D of each compound between bsCAR and mCAR ($p < 0.05$).

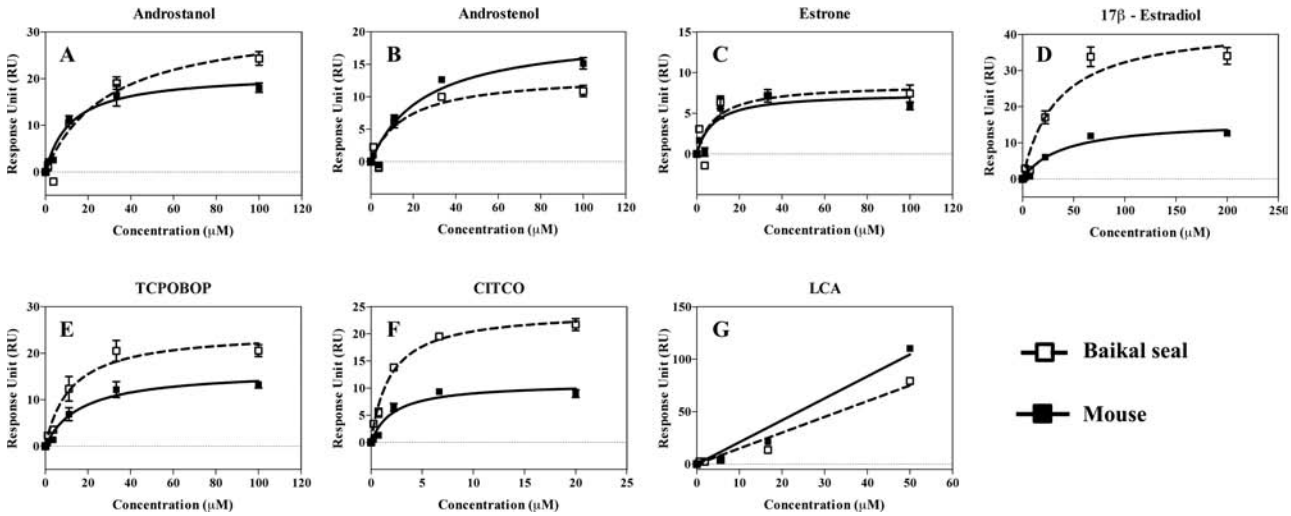

FIG. 2. Results of equilibrium analysis of the direct interaction of chemicals with bsCAR and mCAR LBDs. The data are presented as the mean and SD of triplicate assays.

surface of the sensor chip (Bravman *et al*., 2008). His-tagged bsCAR and mCAR LBDs were immobilized with amine coupling method on the SPR sensor chip under the optimal pH 4.0 of protein dilution buffer. LBD proteins of bsCAR (50 μg/ml) and mCAR (20 μg/ml) were prepared in 10mM sodium acetate buffer (pH 4.0) and injected at a flow rate of 25 μl/min for 12 and 15 min, respectively. The bsCAR and mCAR LBDs were immobilized up to 13,200 and 12,800 RU levels, respectively, which were enough to detect the interaction with small ligands. The interaction of CAR LBD proteins with candidate chemicals was monitored using the optimized SPR biosensor system. The candidate chemicals were selected based on the results from *in vitro* transactivation assay in our previous study (Sakai *et al*., 2006). Results of the CAR interaction for tested compounds are summarized in Table 2 and Figure 2. For checking the reproducibility of the measurements, all the experiments of CAR-ligand interactions were performed at least thrice. The K_D value for each tested chemical was well reproducible, showing a low SD (Table 2).

As expected, androstanol, androstenol, estrone, 17β-estradiol, and TCPOBOP, which are known to be ligands for mCAR (Forman *et al*., 1998; Mäkinen *et al*., 2003; Moore *et al*., 2000; Tzameli *et al*., 2000), showed a specific binding to mCAR LBD (Supplementary fig. S2 A2–E2). Interestingly, these compounds bound to bsCAR (Supplementary fig. S2 A1–E1) although they showed minimal effect on bsCAR transactivation in our previous study (Sakai *et al*., 2006). The binding affinities of these compounds with CAR LBDs were

calculated from the equilibrium analysis, when the responses reached a maximum plateau (Table 2 and Figs. 2A–E). Bile acids including CA, CDCA, DCA, and LCA, for which the action is known to be mediated by CAR and other members of NR1I subfamily (Beilke *et al*., 2009; Renga *et al*., 2011), were also tested. All these bile acids displayed nonspecific binding to bsCAR and mCAR LBDs; even though dose-dependent responses were found, the responses did not reach a plateau (Fig. 2G and Supplementary fig. S2 G1 and G2; only LCA data are shown). These results were mostly consistent with our previous study, in which CA, CDCA, and DCA displayed no or weak activation for bsCAR and mCAR even at 100μM, and LCA had a response only at 100μM (Sakai *et al*., 2006). CITCO that showed responses to hCAR and bsCAR in an *in vitro* transactivation assay (Maglich *et al*., 2003; Sakai *et al*., 2006) also showed binding ability with both bsCAR and mCAR in this study (Fig. 2F and Supplementary fig. S2 F1 and F2). Similar with the results of bile acids, BPA, one of plasticizers that is known to activate hCAR (DeKeyser *et al*., 2011), had a nonspecific binding with bsCAR and mCAR LBDs (data not shown).

Interaction of Ligand-Treated CAR LBD with SRC1. The effects of ligands on the interaction of CAR LBD with SRC1 were detected by the Biacore SPR system, in which SRC1 was initially immobilized on the sensor chip to measure the interaction with ligand-treated CAR LBDs (Fig. 3).

Endogenous ligands, including androstanol, androstenol, estrone, and 17β-estradiol, were examined. Androstanol and androstenol that are known as mCAR antagonists repressed the

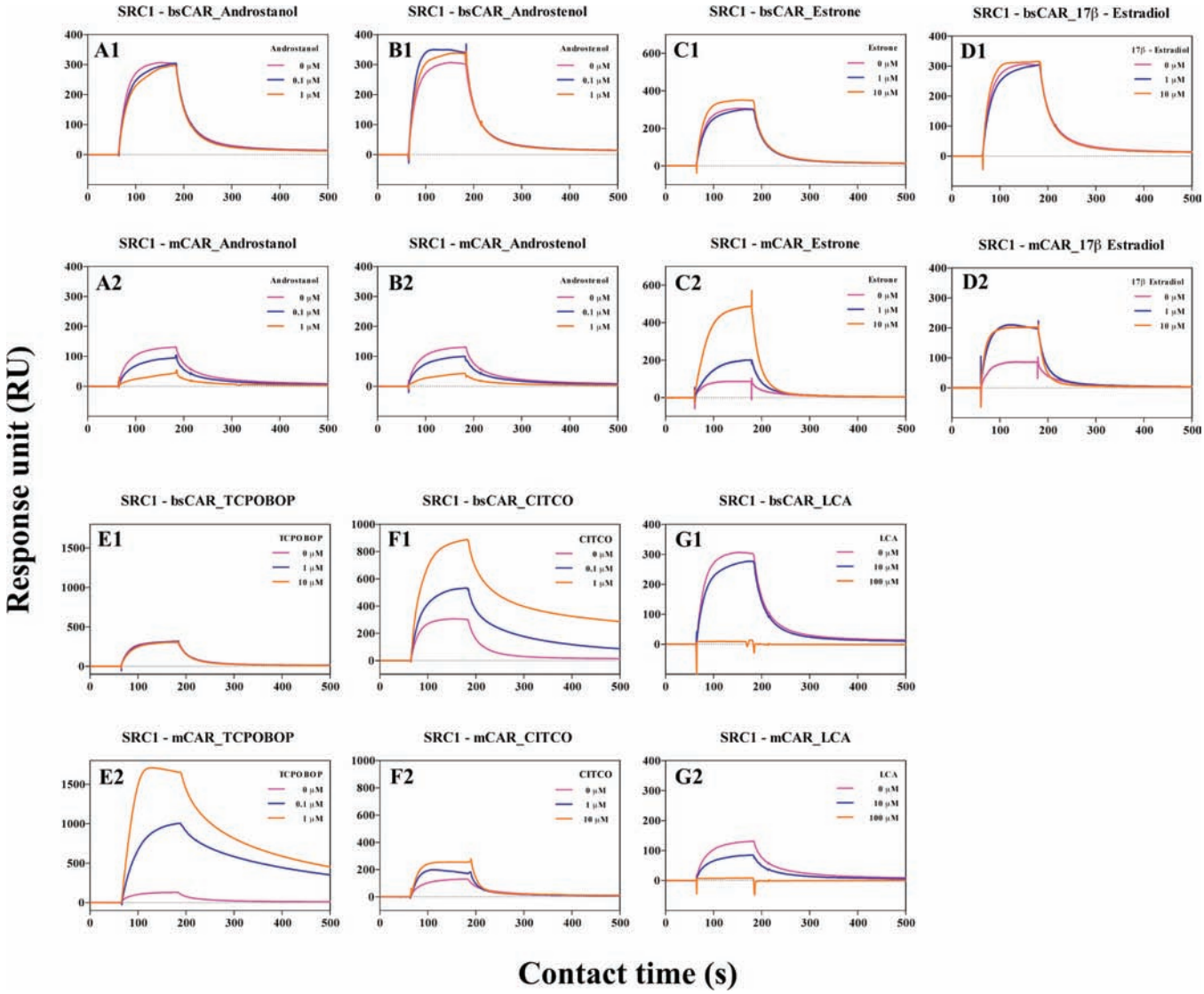

FIG. 3. Results of kinetic analysis of the interaction of SRC1 coactivator with ligand-treated bsCAR and mCAR LBDs. Tested chemicals include (A) androstanol, (B) androstenol, (C) estrone, (D) 17β-estradiol, (E) TCPOBOP, (F) CITCO, and (G) LCA. Sensorgrams for (1) bsCAR and (2) mCAR are shown.

interaction of mCAR with SRC1 in a dose-dependent manner (Figs. 3A2 and B2). These results were consistent with some previous studies indicating that these androstanes suppressed mCAR-mediated constitutive transactivation (Forman *et al*., 1998; Jyrkkärinne *et al*., 2005; Moore *et al*., 2000; Shan *et al*., 2004). In contrast, the interaction of mCAR/SRC1 was dose dependently enhanced during treatment with mCAR agonists, estrone, and 17β-estradiol (Figs. 3C2 and D2), as observed in mCAR transactivation and mCAR/SRC1 interaction assays (Mäkinen *et al*., 2003; Sakai *et al*., 2006). Treatment with TCPOBOP (known as mCAR agonist) also robustly increased the interaction of mCAR LBD with SRC1 in a dose-dependent manner (Fig. 3E2). Intriguingly, consistent with results from our *in vitro* transactivation assay so far reported (Sakai *et al*., 2006), the interaction of bsCAR LBD with SRC1 had no or less effect by the above chemicals (Figs. 3A1–E1). On the other hand, CITCO displayed a stronger induction on bsCAR/SRC1 interaction (Fig. 3F2) but less effect on mCAR/SRC1 interaction (Fig. 3F2). LCA completely repressed the interaction of SRC1 with both bsCAR and mCAR LBDs at 100μM (Figs. 3G1 and G2).

Computational Modeling. To bridge the gap between data from the ligand-binding assay and the coactivator-interaction assay, *in silico* analyses were conducted. To construct a homology model for bsCAR LBD, we applied a crystal structure of hCAR LBD as a template (Xu *et al*., 2004) because they share a 84% amino acid identity (Sakai *et al*., 2006). The homology model of bsCAR LBD bears a close resemblance to hCAR LBD, with a low root-mean square deviation (RMSD) value (0.408Å). The structure of bsCAR LBD was also compared with mCAR LBD (Suino *et al*., 2004) (Fig. 4). The results revealed that bsCAR LBD had a similar secondary structure with mCAR LBD, including eleven α helices, two 3^{10} helices (H2 and H2′), and three small β strands (Figs. 4A and 4B). As reported as distinct features of mCAR and hCAR (Suino *et al*., 2004; Xu *et al*., 2004), bsCAR displayed a short linker region (H11/Hx) between helices H10 and H12/AF2 and also a short

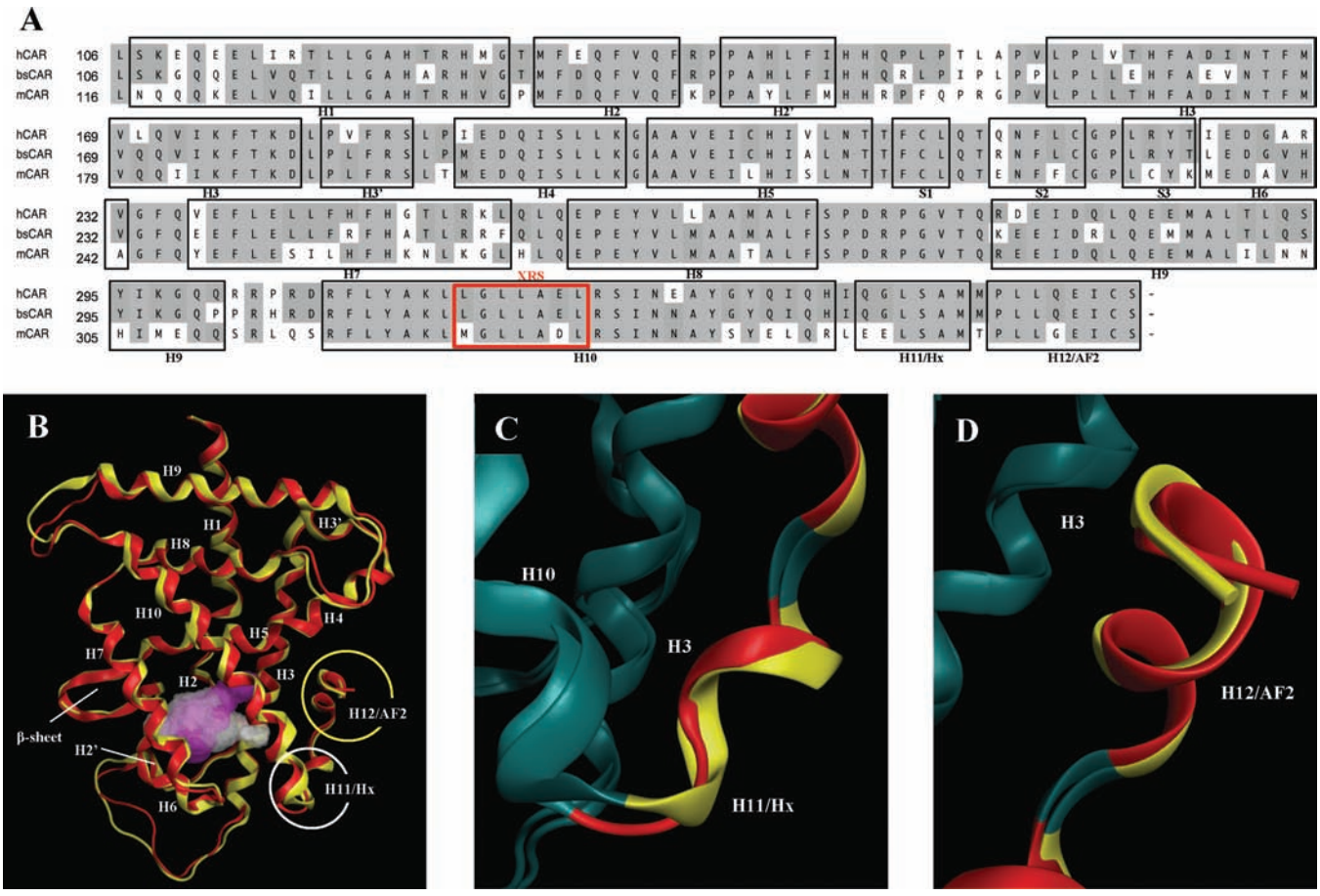

FIG. 4. Amino acid sequences and results of the homology modeling of CAR LBD. (A) Sequence alignment of hCAR, bsCAR, and mCAR LBD. The secondary structural elements are boxed and noted below the sequences. Red box: XRS. (B) Structural comparison between bsCAR LBD and mCAR LBD. bsCAR is colored in red and mCAR is in yellow, and structural elements are noted. LBD structures with LBP of bsCAR (magenta net) and mCAR (white net) were calculated with MOE Atom Region option. The *circle* indicates the helix 11 (white) and 12 (yellow) that are involved in the dimerization and transactivation of CAR, respectively. (C) Detailed views of the helix 11. (D) Detailed views of the helix 12.

H12/AF2 helix (Figs. 4A and 4B). The RMSD value of the Cα atom between the bsCAR LBD and mCAR LBD was 1.08 Å.

The ligand-binding sites and/or ligand-binding pocket (LBP) of mCAR and bsCAR were determined using the MOE Alpha Site Finder. The structural comparison of mCAR and bsCAR was made in the apo structure. The result showed that bsCAR has an almost equal size of the LBP volume as mCAR (666 $Å^3$ for bsCAR and 656 $Å^3$ for mCAR). The LBPs were mainly constituted by hydrophobic residues and only a few hydrophilic residues that belong to helices H3, H4, H5, H6, H7, and H10 and two beta sheets, S2 and S3 (Fig. 4B). The linker helix 11 (helix X) and helix 12 covered one side of the pocket (Figs. 4C and 4D). The main difference between bsCAR and mCAR LBDs was observed in loop regions. Helix 11 of mCAR that can contribute to the dimerization of CAR-RXR (Wright *et al.*, 2011) was replaced by a single turn in bsCAR (Figs. 4A and 4C). A single M340 residue between helix 11 and helix 12 in bsCAR, which effectively limits the conformation freedom of hCAR (Xu *et al.*, 2004), was replaced by T350 in mCAR. Ligand docking with bsCAR or mCAR LBD was conducted for androstenol as an mCAR antagonist (Forman *et al.*, 1998) and TCPOBOP as an mCAR agonist (Tzameli *et al.*, 2000) using ASEDock program. The key amino acids interacting with ligands were then determined by the ligand interaction module of MOE. The result indicated that TCPOBOP and androstenol were completely positioned within the LBP of CARs (Fig. 5). These docking models also exhibit that the corresponding amino acids responsible for the ligand interaction were similar between bsCAR and mCAR. Amino acids including F171, N175, H213, L216, F227, Y234, F244, and Y336 in mCAR

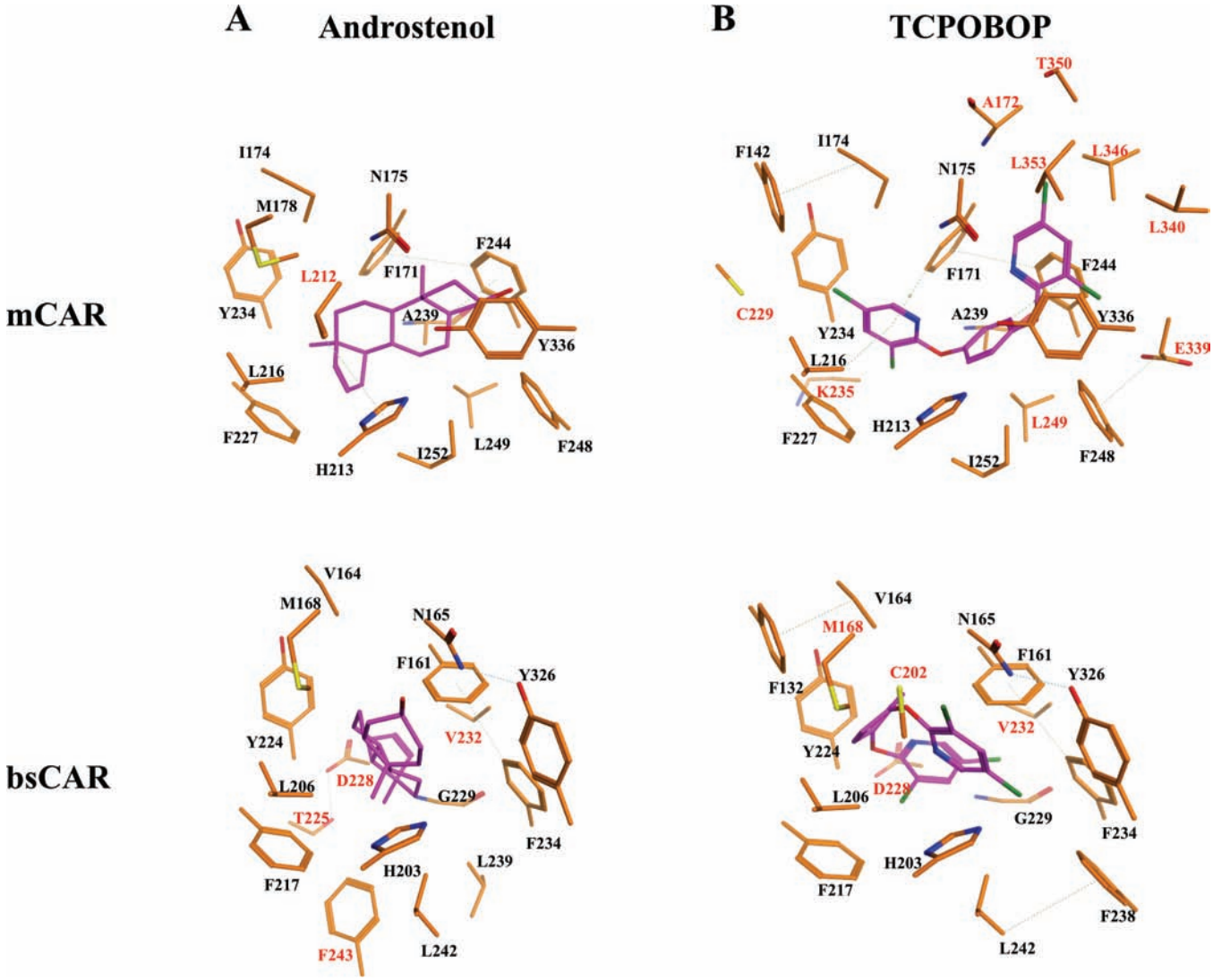

FIG. 5. Predicted binding modes obtained from the docking analysis of (A) androstenol and (B) TCPOBOP for mCAR (top) and bsCAR (bottom) LBD. The ligands are colored in purple and amino acid residues of CAR LBD are shown in gold. The species-specific amino acids are shown in the red letters.

and their corresponding residues in bsCAR rendered in the hydrophobic interaction with TCPOBOP and androstenol. On the other hand, several residues chosen by this docking program were ligand specific; E339, L340, L346, T350, and L353 were involved in the interaction of mCAR with TCPOBOP but not with androstenol. These amino acids were not chosen for the interaction of bsCAR with both TCPOBOP and androstenol.

DISCUSSION

Ligand-Binding Potency of CAR. CAR has a basal transcriptional activity in the absence of ligands but is also able to enhance the transactivation in response to a diverse set of compounds (Forman *et al*., 1998; Huang *et al*., 2003; Kawamoto *et al*., 2000; Wyde *et al*., 2003). Our previous study (Sakai *et al*., 2006) succeeded in isolating CAR cDNA from the Baikal seal. The amino acid sequence of bsCAR LBD shared only 71% identity with mCAR LBD, suggesting that ligand profiles of the CARs are diversified between these two species. Indeed, the transactivation potencies of CAR by endogenous and exogenous compounds were clearly distinct between mCAR, bsCAR (Sakai *et al*., 2006, 2009), and hCAR (Kawamoto *et al*., 2000; Moore *et al*., 2000). Hence, we assumed that the difference in the transactivation potency could be predicted by ligand-CAR binding property. In this study, we attempted to measure the direct binding of ligands with CAR LBDs.

Results on the direct binding of ligands with CAR LBD showed that the tested compounds specifically bound to bsCAR and mCAR with a similar binding affinity across the species although the binding affinities were different among compounds (Table 2). The conserved ligand-binding affinity across the species could not account for the species differences in the CAR-mediated transactivation potencies shown by the ligand treatment in our previous study (Sakai *et al*., 2006). Rather, it might be supported by an equal size of LBP (Fig. 4B) and also by the similarity of amino acid residues in the LBP, especially those related to the ligand interaction of bsCAR and mCAR (Fig. 5). Some of the amino acids (F171, N175, H213, L216, F227, Y234, F244, and Y336) in mCAR are shared with those in bsCAR for the interaction with androstenol and TCPOBOP (Fig. 5), and their important role has also been reported in previous studies (Shan *et al*., 2004; Suino *et al*., 2004).

Our results revealed that bile acids were not specific ligands for CARs, even if bile acids like LCA were found to show a weak transactivation potency of DR4 response element in MCF-7 cells in our previous study (Sakai *et al*., 2006). Although the mechanism for the nonspecific binding of bile acids to CARs remains unknown, it might be due to the cumbersome structure of these compounds. The addition of a 5C side chain on steroid structure may cause difficulty to thrust into the LBP in comparison with steroid hormones. In fact, the molar volumes of bile acids are larger than those of other chemicals examined in this study (Table 1). For example, the molar volume of LCA (351 cm^3/mol) is 1.5 times larger than that of 17β-estradiol (233 cm^3/mol). Moreover, results of the molecular volume of some tested ligands estimated using MD simulation also support this relationship; the molecular volume of LCA (399 $Å^3$) is 1.4 times larger than that of 17β-estradiol (278 $Å^3$). It has also been reported that these compounds are ligands for receptors other than CAR such as pregnane X receptor (PXR) and vitamin D receptor (VDR) (Parks *et al*., 1999). We have suggested that VDR and PXR that are endogenously expressed in MCF-7 may be responsible for the transactivation of DR4 response element by bile acids (Sakai *et al*., 2006). In the transactivation assay, reporter gene activities were actually enhanced by the treatment of some bile acids even in MCF-7 cells with no CAR transfection (Sakai *et al*., 2006). Given these previous results, it is possible to assume that bile acids have no binding potential to activate CAR but can transactivate luciferase gene through VDR and/or PXR. BPA, which has a smaller molar volume (200 cm^3/mol) and molecular volume (238 $Å^3$) than other tested compounds (Table 1), also showed a nonspecific binding with CARs. Although the reason remains unclear, it is likely that BPA fills less of the CAR LBP and binds not only LBP but also other sites.

Effects of Ligands on the Interaction of CAR/SRC1. One might think that the similarity in binding affinities of ligands to bsCAR and mCAR may lead to comparable transcriptional responses through these ligand-activated receptors. However, our present and previous studies indicated that the potential of ligand binding was not reflected in CAR-mediated transactivation. Our ligand-binding assay showed androstanol, androstenol, estrone, 17β-estradiol, and TCPOBOP bound similarly to both bsCAR and mCAR LBDs, whereas these compounds had less or no effect on bsCAR-mediated transactivation, but had apparent effects on mCAR-mediated transactivation, as reported in Sakai *et al*. (2006) (Table 2). The difference in ligand profile between the present direct binding assay and transactivation assay suggests that the critical amino acids involved in the CAR-mediated transactivation are not necessarily the same as those in the ligand binding of CAR. These data also suggest the participation of cofactors in the CAR transcriptional activity, as documented in some previous studies (Forman *et al*., 1998; Jyrkkärinne *et al*., 2005; Leo and Chen, 2000; Maglich *et al*., 2003; Moore *et al*., 2000; Suino *et al*., 2004; Tzameli *et al*., 2000). In this study, we thus investigated the interaction of SRC1 coactivator with ligand-treated CAR LBDs of the Baikal seal and the mouse.

The CAR/SRC1 interaction assay manifested a clear difference between the Baikal seal and the mouse (Fig. 3). The results of androstanol, androstenol, estrone, 17β-estradiol, TCPOBOP, and CITCO agreed well with those of our *in vitro* transactivation assay (Sakai *et al*., 2006) (Table 2). For mCAR LBD, androstanol and androstenol that repressed mCAR transactivation inhibited the interaction with SRC1 in this and other studies (Forman *et al*., 1998; Jyrkkärinne

et al., 2003; Mäkinen *et al*., 2003; Moore *et al*., 2000; Repo *et al*., 2008). Estrone, estradiol, and TCPOBOP effectively enhanced the interaction of SRC1 with mCAR in this study and were able to induce the transactivation through this receptor (Sakai *et al*., 2006), which were consistent with those of other mCAR-driven transactivation and mCAR/SRC1 assays (Jyrkkärinne *et al*., 2003; Mäkinen *et al*., 2003; Repo *et al*., 2008; Tzameli *et al*., 2000). In contrast, for bsCAR LBD, all the three compounds had low or no dose-dependent effect on the interaction with SRC1. These results account for no transactivation potency of bsCAR by the treatment with these compounds (Sakai *et al*., 2006).

Previous studies demonstrated that AF2 domain, a strictly ligand-dependent activation domain located at the C-terminal in LBD (Durand *et al*., 1994), plays an important role in the recruitment of coactivators and corepressors (Jyrkkärinne *et al*., 2005; Mäkinen *et al*., 2003). Accordingly, the difference of residues in the AF2 domain in addition to the ligand binding to CAR can result in the difference in the interaction of CAR/SRC1 through the conformational change of AF2 domain. The comparison of bsCAR and mCAR LBDs indicates that G354 in the AF2 domain of mCAR is Q344 in the corresponding residue of bsCAR (Fig. 4A), and the sequence difference produces the structural difference (Fig. 4D). This finding is in agreement with a previous suggestion (Moore *et al*., 2000); one amino acid substitution (G354 vs. Q344) in the AF2 domain might be responsible for the difference in the *in vitro* transactivation potency between mCAR and hCAR treated with TCPOBOP. In addition, the replacement of L340/L343 in the helix 10 of mCAR by I330/I333 in hCAR and bsCAR (Fig. 4A) and the resulting structural difference (Fig. 4C) may be associated with no effect of TCPOBOP on the recruitment of SRC1, and no dose-dependent transactivation mediated by hCAR (Moore *et al*., 2000) and bsCAR (Sakai *et al*., 2006). Tzameli *et al*. (2000) suggested that I174 in helix 3 of mCAR that makes a specific contact with ligands may affect the interaction with SRC1. The sequence alignment revealed that corresponding residue of the I174 in mCAR was I164 in hCAR, but V164 in bsCAR (Fig. 4A). Remarkably, androstanol had the same repressive effect on both hCAR- and mCAR-mediated transactivation (Moore *et al*., 2000) but had no effect on bsCAR-mediated transactivation (Sakai *et al*., 2006). These findings together with our results suggest that V164 in bsCAR might be a cause of the nonresponse by androstanol. As for LCA, the SRC1 interaction dose dependently decreased for bsCAR and mCAR, while both CARs showed nonspecific binding to this compound. This implies that the nonspecific binding may lead to the conformational change of CAR and suppress the CAR-SRC1 interaction.

Consequently, our results revealed that both of bsCAR and mCAR bind similarly with ligands but interact with SRC1 in a species-specific manner; both events do not necessarily occur in parallel. The transactivation regulation of CAR by its nuclear localization, together with the CAR/SRC1 interaction, may be one of factors for the species-specific responses to chemicals. Zelko *et al*. (2001) recognized that hCAR nuclear translocation is regulated by the xenochemical response signal (XRS) containing amino acids 313–319 in helix 10, and the mutation of L313A abolishes the nuclear translocation. Hence, the difference in amino acids (L313 in hCAR and bsCAR, and M323 in mCAR) among species (Fig. 4A) may also cause the different intracellular behavior of hCAR and bsCAR from that of mCAR and result in the species-specific transactivation potency of CAR.

Computational Modeling. We suggest that our *in silico* docking models may be accurate in defining the ligand-binding ability because the predicted similar structure and size of the LBP between bsCAR and mCAR are well explained by the similar binding affinities with tested chemicals in both the CARs that were found in the SPR assay.

Our sequence alignment and *in silico* analysis also suggest that the differences in amino acid sequences of the CARs support the difference in the *in vitro* transactivation between bsCAR and mCAR. The direct specific binding of TCPOBOP with mCAR LBD observed in our *in vitro* assay is consistent with the result of previous studies (Suino *et al*., 2004; Wright *et al*., 2011). Our *in silico* analysis exhibited a model for the interaction of TCPOBOP and mCAR LBD similar to that in a previous study (Suino *et al*., 2004); the A-ring of TCPOBOP is sandwiched between mCAR Y234 and F227 and the C-ring between Y336 and F244. The C-ring posed direct interaction with L353 of mCAR AF2 domain and with L346 and T350 of the linker helix (Fig. 5B). Extensive hydrophobic interactions between TCPOBOP and mCAR LBD may generate the stabilization of AF2 and linker helix 11 to the state of active conformation by docking TCPOBOP (Fig. 5B), leading to a ligand-dependent allosteric regulation of mCAR transactivation by prompting SRC1 recruitment (Suino *et al*., 2004; Wright *et al*., 2011). On the other hand, the specific binding of TCPOBOP with bsCAR LBD was unexpected even though our earlier study showed no dose-dependent transactivation in bsCAR-driven reporter gene assay (Sakai *et al*., 2006). This may be explained by our *in silico* analysis in which no interaction of TCPOBOP with amino acids in the AF2 and linker helix 11 was observed in bsCAR (Fig. 5B). This may be because T350, which makes direct interaction with C-ring of TCPOBOP in mCAR, is replaced by M340 in bsCAR. The same replacement (M340) occurs in hCAR (Fig. 4A) and explains no TCPOBOP-mediated activation of hCAR (Moore *et al*., 2000). A recent study proposed 339–345 amino acid residues (ELQRLEE) in mCAR as the allosteric regulatory site (Wright *et al*., 2011). Intriguingly, the corresponding site in bsCAR and hCAR (329–335; QIQHIQG) is poorly conserved (Fig. 4A). These results imply no TCPOBOP-induced allosteric regulation in bsCAR. Hence, we suggest that the structural differences in helices 11 and 12 between bsCAR and mCAR may be responsible for the different ligand-dependent interaction with SRC1 and further species-specific transactivation.

Jyrkkärinne *et al*. (2003) suggested that amino acids 201–263 (helices 5–7) of mCAR contribute to the response to androstenol. Because this region is poorly conserved among the mouse, human, and Baikal seal (Fig. 4A), this may be one of the reasons accounting for the differences in CAR-mediated responses in these species. Our androstenol docking analysis identified T225, D228, V232, and F243 in bsCAR helices 5–7 as unique amino acids that may be involved in the docking of this ligand (Fig. 5A). However, three (T225, V232, and F243) out of the four amino acids are not conserved in mCAR (K235, A242, and L253, respectively). Hence, we assume that these amino acids may contribute to no antagonistic effect of androstenol on bsCAR-mediated transactivation.

In this study, the structure of bsCAR was made in the apo structure without ligands. However, the disordered loop regions in helices 11 and 12 would not be due to the lack of RXR, coactivator, and ligand. As the template of hCAR that we used to construct the homology model of bsCAR has been generated based on CAR/RXR LBD heterodimer bound to CITCO and a SRC1 peptide, the basic structure of the loop region of bsCAR should be mostly conserved as the template of hCAR.

In summary, this study revealed that the binding affinities of ligands to CAR LBD were similar for the Baikal seal and the mouse, but the interactions of ligand-treated CAR LBDs with SRC1 were species specific. The results of ligand-dependent CAR/SRC1 interaction assay accounted for those of the *in vitro* transactivation assay that was conducted in our previous study. Overall, this suggests that the ligand binding of CAR is a necessary initial step for the enhanced transactivation over the constitutive level, but not sufficient. The interaction with coactivators is critical for ligand-dependent CAR transactivation in a species-specific manner. The present study demonstrated that our SPR system could detect the binding of small molecules (< 500 kD) to CAR protein that was immobilized on the sensor chip. Our findings also show that the ligand affinity to CAR varied among compounds. These results demonstrate that this SPR system can be a valuable tool for high-throughput screening of potential CAR ligands and also can aid to assess the risk of these compounds.

SUPPLEMENTARY DATA

Supplementary data are available online at http://toxsci.oxfordjournals.org/.

FUNDING

Grant-in-Aid for Scientific Research (S) [No. 21221004] from the Japan Society for the Promotion of Science and "Global COE Program" from the Ministry of Education, Culture, Sports, Science and Technology, Japan. Financial assistance was also provided in part by Basic Research in ExTEND2005 (Enhanced Tack on Endocrine Disruption) from the Ministry of Environment, Japan. This research was also supported by the Basic Science Research Program through the National Research Foundation of Korea funded by the Ministry of Education, Science and Technology to E.-Y.K. (20110004230, 20110003337).

ACKNOWLEDGMENTS

The authors would like to thank Dr Tesuro Agusa, Ehime University, for the technical assistance and Prof. An. Subramanian, Ehime University, for the critical reading of this manuscript.

REFERENCES

Assem, M., Schuetz, E. G., Leggas, M., Sun, D., Yasuda, K., Reid, G., Zelcer, N., Adachi, M., Strom, S., Evans, R. M., *et al.* (2004). Interactions between hepatic Mrp4 and Sult2a as revealed by the constitutive androstane receptor and Mrp4 knockout mice. *J. Biol. Chem.* **279,** 22250–22257.

Baes, M., Gulick, T., Choi, H. S., Martinoli, M. G., Simha, D., and Moore, D. D. (1994). A new orphan member of the nuclear hormone receptor superfamily that interacts with a subset of retinoic acid response elements. *Mol. Cell. Biol.* **14,** 1544–1552.

Beilke, L. D., Aleksunes, L. M., Olson, E. R., Besselsen, D. G., Klaassen, C. D., Dvorak, K., and Cherrington, N. J. (2009). Decreased apoptosis during CAR-mediated hepatoprotection against lithocholic acid-induced liver injury in mice. *Toxicol. Lett.* **188,** 38–44.

Bravman, T., Bronner, V., Nahshol, O., and Schreiber, G. (2008). The ProteOn XPR36™ array system-high throughput kinetic binding analysis of biomolecular interactions. *Cell. Mol. Bioeng*. **1,** 216–228.

DeKeyser, J. G., Laurenzana, E. M., Peterson, E. C., Chen, T., and Omiecinski, C. J. (2011). Selective phthalate activation of naturally occurring human constitutive androstane receptor splice variants and the pregnane X receptor. *Toxicol. Sci.* **120,** 381–391.

Dong, B., Saha, P. K., Huang, W., Chen, W., Abu-Elheiga, L. A., Wakil, S. J., Stevens, R. D., Ilkayeva, O., Newgard, C. B., Chan, L., *et al.* (2009). Activation of nuclear receptor CAR ameliorates diabetes and fatty liver disease. *Proc. Natl. Acad. Sci. U.S.A.* **106,** 18831–18836.

Durand, B., Saunders, M., Gaudon, C., Roy, B., Losson, R., and Chambon, P. (1994). Activation function 2 (AF-2) of retinoic acid receptor and 9-*cis* retinoic acid receptor: Presence of a conserved autonomous constitutive activating domain and influence of the nature of the response element on AF-2 activity. *EMBO J.* **13,** 5370–5382.

Endo, Y., and Sawasaki, T. (2003). High-throughput, genome-scale protein production method based on the wheat germ cell-free expression system. *Biotechnol. Adv.* **21,** 695–713.

Forman, B. M., Tzameli, I., Choi, H. S., Chen, J., Simha, D., Seol, W., Evans, R. M., and Moore, D. D. (1998). Androstane metabolites bind to and deactivate the nuclear receptor CAR-beta. *Nature* **395,** 612–615.

Halgren, T. A. (1996). Merck molecular force field. I. Basis, form, scope, parameterization, and performance of MMFF94. *J. Comput. Chem*. **17,** 490–519.

Honkakoski, P., Zelko, I., Sueyoshi, T., and Negishi, M. (1998). The nuclear orphan receptor CAR-retinoid X receptor heterodimer activates the phenobarbital-responsive enhancer module of the *CYP2B* gene. *Mol. Cell. Biol.* **18,** 5652–5658.

Huang, W., Zhang, J., Chua, S. S., Qatanani, M., Han, Y., Granata, R., and Moore, D. D. (2003). Induction of bilirubin clearance by the constitutive androstane receptor (CAR). *Proc. Natl. Acad. Sci. U.S.A.* **100,** 4156–4161.

Huang, W., Zhang, J., Washington, M., Liu, J., Parant, J. M., Lozano, G., and Moore, D. D. (2005). Xenobiotic stress induces hepatomegaly and liver tumors via the nuclear receptor constitutive androstane receptor. *Mol. Endocrinol.* **19,** 1646–1653.

Imaeda, D., Kunisue, T., Ochi, Y., Iwata, H., Tsydenova, O., Takahashi, S., Amano, M., Petrov, E. A., Batoev, V. B., and Tanabe, S. (2009). Accumulation features and temporal trends of PCDDs, PCDFs and PCBs in Baikal seals (*Pusa sibirica*). *Environ. Pollut.* **157,** 737–747.

Iwata, H., Watanabe, M., Okajima, Y., Tanabe, S., Amano, M., Miyazaki, N., and Petrov, E. A. (2004). Toxicokinetics of PCDD, PCDF, and coplanar PCB congeners in Baikal seals, *Pusa sibirica*: Age-related accumulation, maternal transfer, and hepatic sequestration. *Environ. Sci. Technol.* **38,** 3505–3513.

Jyrkkärinne, J., Mäkinen, J., Gynther, J., Savolainen, H., Poso, A., and Honkakoski, P. (2003). Molecular determinants of steroid inhibition for the mouse constitutive androstane receptor. *J. Med. Chem.* **46,** 4687–4695.

Jyrkkärinne, J., Windshügel, B., Mäkinen, J., Ylisirniö, M., Peräkylä, M., Poso, A., Sippl, W., and Honkakoski, P. (2005). Amino acids important for ligand specificity of the human constitutive androstane receptor. *J. Biol. Chem.* **280,** 5960–5971.

Kanno, Y., and Inouye, Y. (2008). Molecular basis of the intracellular localization of the constitutive androstane receptor (CAR). *J. Health Sci*. **54,** 261–266.

Kawamoto, T., Kakizaki, S., Yoshinari, K., and Negishi, M. (2000). Estrogen activation of the nuclear orphan receptor CAR (constitutive active receptor) in induction of the mouse *Cyp2b10* gene. *Mol. Endocrinol.* **14,** 1897–1905.

Kawamoto, T., Sueyoshi, T., Zelko, I., Moore, R., Washburn, K., and Negishi, M. (1999). Phenobarbital-responsive nuclear translocation of the receptor CAR in induction of the *CYP2B* gene. *Mol. Cell. Biol.* **19,** 6318–6322.

Leo, C., and Chen, J. D. (2000). The SRC family of nuclear receptor coactivators. *Gene* **245,** 1–11.

Maglich, J. M., Parks, D. J., Moore, L. B., Collins, J. L., Goodwin, B., Billin, A. N., Stoltz, C. A., Kliewer, S. A., Lambert, M. H., Willson, T. M., *et al.* (2003). Identification of a novel human constitutive androstane receptor (CAR) agonist and its use in the identification of CAR target genes. *J. Biol. Chem.* **278,** 17277–17283.

Mäkinen, J., Reinisalo, M., Niemi, K., Viitala, P., Jyrkkärinne, J., Chung, H., Pelkonen, O., and Honkakoski, P. (2003). Dual action of oestrogens on the mouse constitutive androstane receptor. *Biochem. J.* **376**(Pt 2), 465–472.

Masi, A. D., Marinis, E. D., Ascenzi, P., and Marino, M. (2009). Nuclear receptors CAR and PXR: Molecular, functional, and biomedical aspects. *Mol. Asp. Med*. **30,** 297–343.

Moore, L. B., Parks, D. J., Jones, S. A., Bledsoe, R. K., Consler, T. G., Stimmel, J. B., Goodwin, B., Liddle, C., Blanchard, S. G., Willson, T. M., *et al.* (2000). Orphan nuclear receptors constitutive androstane receptor and pregnane X receptor share xenobiotic and steroid ligands. *J. Biol. Chem.* **275,** 15122–15127.

Parks, D. J., Blanchard, S. G., Bledsoe, R. K., Chandra, G., Consler, T. G., Kliewer, S. A., Stimmel, J. B., Willson, T. M., Zavacki, A. M., Moore, D. D., *et al.* (1999). Bile acids: Natural ligands for an orphan nuclear receptor. *Science* **284,** 1365–1368.

Qatanani, M., Zhang, J., and Moore, D. D. (2005). Role of the constitutive androstane receptor in xenobiotic-induced thyroid hormone metabolism. *Endocrinology* **146,** 995–1002.

Renga, B., Migliorati, M., Mencarelli, A., Cipriani, S., D'Amore, C., Distrutti, E., and Fiorucci, S. (2011). Farnesoid X receptor suppresses constitutive androstane receptor activity at the multidrug resistance protein-4 promoter. *Biochim. Biophys. Acta* **1809,** 157–165.

Repo, S., Jyrkkärinne, J., Pulkkinen, J. T., Laatikainen, R., Honkakoski, P., and Johnson, M. S. (2008). Ligand specificity of constitutive androstane receptor as probed by induced-fit docking and mutagenesis. *J. Med. Chem.* **51,** 7119–7131.

Rich, R. L., Hoth, L. R., Geoghegan, K. F., Brown, T. A., LeMotte, P. K., Simons, S. P., Hensley, P., and Myszka, D. G. (2002). Kinetic analysis of estrogen receptor/ligand interactions. *Proc. Natl. Acad. Sci. U.S.A.* **99,** 8562–8567.

Sakai, H., Iwata, H., Kim, E. Y., Tsydenova, O., Miyazaki, N., Petrov, E. A., Batoev, V. B., and Tanabe, S. (2006). Constitutive androstane receptor (CAR) as a potential sensing biomarker of persistent organic pollutants (POPs) in aquatic mammal: Molecular characterization, expression level, and ligand profiling in Baikal seal (*Pusa sibirica*). *Toxicol. Sci.* **94,** 57–70.

Sakai, H., Kim, E. Y., Petrov, E. A., Tanabe, S., and Iwata, H. (2009). Transactivation potencies of Baikal seal constitutive active/androstane receptor by persistent organic pollutants and brominated flame retardants. *Environ. Sci. Technol.* **43,** 6391–6397.

Sawasaki, T., Hasegawa, Y., Tsuchimochi, M., Kamura, N., Ogasawara, T., Kuroita, T., and Endo, Y. (2002). A bilayer cell-free protein synthesis system for high-throughput screening of gene products. *FEBS Lett.* **514,** 102–105.

Shan, L., Vincent, J., Brunzelle, J. S., Dussault, I., Lin, M., Ianculescu, I., Sherman, M. A., Forman, B. M., and Fernandez, E. J. (2004). Structure of the murine constitutive androstane receptor complexed to androstenol: A molecular basis for inverse agonism. *Mol. Cell* **16,** 907–917.

Suino, K., Peng, L., Reynolds, R., Li, Y., Cha, J. Y., Repa, J. J., Kliewer, S. A., and Xu, H. E. (2004). The nuclear xenobiotic receptor CAR: Structural determinants of constitutive activation and heterodimerization. *Mol. Cell* **16,** 893–905.

Turner, B., Tabul, M., and Nimri, S. (2008). Applications of the ProteON GLH sensor chip: Interactions between proteins and small molecules. *Bio-Rad Tech Note* 5679.

Tzameli, I., Pissios, P., Schuetz, E. G., and Moore, D. D. (2000). The xenobiotic compound 1,4-bis[2-(3,5-dichloropyridyloxy)]benzene is an agonist ligand for the nuclear receptor CAR. *Mol. Cell. Biol.* **20,** 2951–2958.

Wang, J., Cieplak, P., and Kollman, P. (2000). How well does a restrained electrostatic potential (RESP) model perform in calculating conformational energies of organic and biological molecules? *J. Comput. Chem*. **21,** 1049–1074.

Wright, E., Busby, S. A., Wisecarver, S., Vincent, J., Griffin, P. R., and Fernandez, E. J. (2011). Helix 11 dynamics is critical for constitutive androstane receptor activity. *Structure* **19,** 37–44.

Wyde, M. E., Bartolucci, E., Ueda, A., Zhang, H., Yan, B., Negishi, M., and You, L. (2003). The environmental pollutant 1,1-dichloro-2,2-bis (*p*-chlorophenyl)ethylene induces rat hepatic cytochrome P450 2B and 3A expression through the constitutive androstane receptor and pregnane X receptor. *Mol. Pharmacol.* **64,** 474–481.

Xu, R. X., Lambert, M. H., Wisely, B. B., Warren, E. N., Weinert, E. E., Waitt, G. M., Williams, J. D., Collins, J. L., Moore, L. B., Willson, T. M., *et al.* (2004). A structural basis for constitutive activity in the human CAR/RXRalpha heterodimer. *Mol. Cell* **16,** 919–928.

Yamamoto, Y., Moore, R., Goldsworthy, T. L., Negishi, M., and Maronpot, R. R. (2004). The orphan nuclear receptor constitutive active/androstane receptor is essential for liver tumor promotion by phenobarbital in mice. *Cancer Res.* **64,** 7197–7200.

Zelko, I., Sueyoshi, T., Kawamoto, T., Moore, R., and Negishi, M. (2001). The peptide near the C terminus regulates receptor CAR nuclear translocation induced by xenochemicals in mouse liver. *Mol. Cell. Biol.* **21,** 2838–2846.